

Extract from *Clarias batrachus* Fins as Environmental Benign Corrosion Inhibitor for Mild Steel in Acidic Solution

Shivani Singh¹, Rahul Singh^{1,*}, Neeta Raj Sharma^{1,*}, Ambrish Singh^{2,*}

¹ School of Bioengineering and Biosciences, Lovely Professional University, Phagwara, Punjab, India-144402.

² School of New Energy and Materials, Southwest Petroleum University, Chengdu-610500, Sichuan, China.

*E-mail:neeta.raj@lpu.co.in; rahul.16188@lpu.co.in; vishisingh4uall@gmail.com

Received: 23 November 2021/ Accepted: 12 January 2022 / Published: 2 February 2022

Extract of *Clarias batrachus* fins (ECBF) was prepared and detached to solution to prevent mild steel from corroding in 0.5M sulfuric acid. Gravimetric (weight loss), electrochemical, and exterior characterization experiments were used to investigate the process. As the inhibitor concentration was increased, weight loss tests exposed a boost in inhibition effectiveness and a decrease in corrosion rate. Impedance studies suggested a maximum inhibition efficacy of 95.8% was achieved with 600 mg/L of ECBF inhibitor in corrosive media. Electrochemical frequency modulation (EFM) revealed that the casualty factors 2, 3 are consistent with theoretical values, and ECBF is more efficient than blank (0.5M H₂SO₄). The polarization data revealed that the ECBF inhibitor was predominantly cathodic. The ECBF layer generation on the steel surface was discovered using scanning electron microscopy (SEM) and atomic force microscopy (AFM).

Keywords: Mild steel; *Clarias batrachus*; Electrochemical; Corrosion; EFM; AFM

1. INTRODUCTION

Corrosion of metals and alloys is a global problem causing accidents, deaths, shut downs, and economic losses. It is an interdisciplinary phenomenon and is connected to various systems. It has become part and parcel of metals and alloys in different environments. Several groups are working day and night to provide solutions to mitigate corrosion. But, still the methods used or available nowadays are not able to stop it fully or are very expensive. Due to the demand and use of metals in several industries, it is always a concern in order to avoid failures and operational shutdowns [1-5].

Mild steel is used in industries commonly due to its cheapness and good tensile strength. Acids and extreme corrosive environments can cause the mild steel to corrode easily. Several methods are

employed to mitigate the corrosion of mild steel in acidic solution. Use of inhibitors is one of them that can effectively mitigate the corrosion of mild steel. Various inhibitors including organic, inorganic, vapor phase, drugs, and plant extracts have been used [6-10] to delay corrosion. But, there is always a need to develop and test new, cheap, and sustainable inhibitors due to existing demand and environmental regulations. The current work is an interdisciplinary work of its own kind reported for the first time. Extract of *Clarias batrachus* fins (ECBF) were tested as a promising corrosion inhibitor with regards to regulations and waste management [6-10]. The idea was developed after watching a TV documentary where people were drinking soup made from shark's fin (an expensive drink). So, preliminary tests were carried out to see whether ECBF is suitable for mild steel in acidic solution. ECBF gave good results and further tests were carried out to confirm its potential and provide a good solution to industries. ECBF is eco-friendly and is made from the waste products (fins) of *Clarias batrachus* that people usually throw after consuming the fish.

Clarias batrachus, popularly known as Mangur or Catfish, is an Asian native and one of the most delectable meals eaten by humans owing to its protein-rich and delicious flesh. It may be found from the eocene to the recent in Asian nations such as India, Myanmar, Sri Lanka, Malaya, and the Archipelago. It is medicinally significant, and most doctors suggest it for a variety of disorders, including tuberculosis (TB). *Clarias batrachus* is known as the catfish because it has whiskers or barbels on each side of its mouth that resembles those of a cat (Fig.1). It may be found in natural ponds, pools, ditches, and other shallow water resources, and it is a scavenger. It breeds during the rainy season and can live in water with very little oxygen. Fresh and brackish water are the most common habitats for this species. Clams, bug larvae, and tiny crustaceans are among its favorite foods.

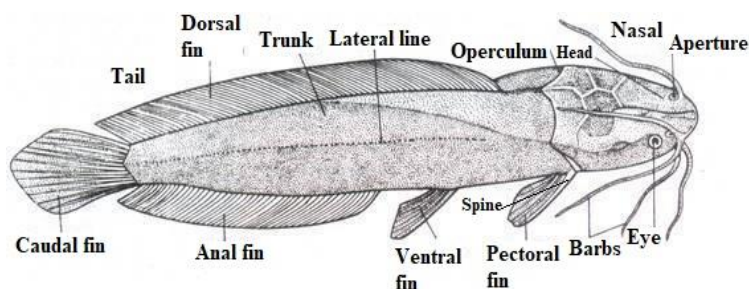


Figure 1. Graphical representation of body parts of *Clarias batrachus*.

2. EXPERIMENTAL PROCESSES

2.1. Inhibitor

The *Clarias batrachus* fins depicted in Figure 2 were gathered from a reservoir on the outskirts of Varanasi, Uttar Pradesh, India. Five days in the sun dried the anal, ventral, pectoral, and dorsal and caudal fins off the fish. A mixer grinder was used to ground the dry fins. The dried fins were ground into a fine powder and ethanol was added to the mixture to extract the oil. The sulfuric acid solution

was used to reflux and then concentrate the extracted solution for corrosion experiments. This solution was further diluted to different concentrations of 50, 100, 200, 400 and 600 mg/l that were used in the acidic solution.



Figure 2. Different fins of *Clarias batrachus*.

2.2. Materials

It was necessary to fuse copper wire to one end of the mild steel electrode, which was then covered with epoxy resin. In preparation for each experiment, a 1cm² surface was abraded using silicon sheets that had different pore sizes on them. In an ultrasonic tank, the electrode was cleaned with a solution of water, acetone, and ethyl alcohol. To ensure that there was no water on the steel electrode, it was vacuum dried. 0.5M sulfuric acid solution, arranged from absolute sulfuric acid and distilled water, was used in all of the assays.

2.3. Gravimetric analysis

ASTM G31-2004 [11] was used to conduct the gravimetric tests. To prepare the mild steel coupons for vacuum drying, they were soaked in Clarke's solution and water. Various quantities of ECBF in sulfuric acid were used to immerse the coupons. There were two methods used to measure and record mild steel's weight loss: blank and inhibited. The corrosion rate was calculated using these weight loss parameters. The mean results of each test were evaluated to ensure repeatability. The corrosion rate was calculated using the following equation:

$$C_R = \frac{8.76 \times 10^4 \times W}{a \times t \times \rho} \quad (1)$$

where W be the weight loss of steel (mg), a be the area of steel, t be the immersion time (h), and ρ be the density of steel (g·cm⁻³).

2.4. Electrochemical Research

Impedance, frequency modulation, and polarization approaches were all tested using a Gamry digital system with three electrode assemblies. Typical electrochemical equipment includes a reference electrode made of Ag/AgCl, a counter electrode made of graphite, and a working electrode made of mild steel. Preparation time was required for each exam before it could begin. The standard deviations of the findings are shown for each test that was carried out three times. Using the equations below, the inhibition efficiency from impedance and polarization tests was calculated:

$$\eta_{EIS} = \frac{R_{(inh)} - R}{R_{(inh)}} \times 100 \quad (2)$$

$$\eta_{PDP} = \frac{i_{corr} - i_{corr(inh)}}{i_{corr}} \times 100 \quad (3)$$

where R be charge transfer resistance of the sulfuric acid and $R_{(inh)}$ be the charge transfer resistance of ECBF inhibitor in sulfuric acid, respectively. i_{corr} represents the current density of sulfuric acid and $i_{corr(inh)}$ represents the current density of ECBF inhibitor in sulfuric acid, respectively [13].

Experimental investigations of electrochemical frequency modulation (EFM) were carried out at amplitudes of 10 mV with frequencies of 2 and 5 Hz [14, 15], and the results were published. When it comes to assessing the corrosion rate in a short period of time, this approach is quite useful.

2.5. Surface analyses

For each steel surface evaluation, the samples were submerged in 0.5M sulfuric acid solution without and with ECBF inhibitor in the Ziess Evo 50 XVP apparatus for scanning electron microscopy (SEM) testing. In order to determine the roughness of mild steel surfaces on a number of specimens, the Dimension Icon Brock instrument was used. To create 3D figures, all of the 2D photos collected after the research were uploaded to the Nanoscope analysis programme, which then processed them.

3. RESULTS AND DISCUSSION

3.1. Gravimetric tests

A concentration versus inhibition efficiency graphic depicts the effect of ECBF concentrations on the preventive masking of steel surfaces (Fig. 3).

As demonstrated in the figure, the moderating effect of ECBF inhibitor rises with increasing concentration, reaching a maximum effectiveness of 95% at 600 mg/L. Corrosion rate, on the other hand, decreases when inhibitor concentration increases. The ECBF molecules' adsorption into a large area of the steel surface improved mitigation ability and reduced corrosion rate [15].

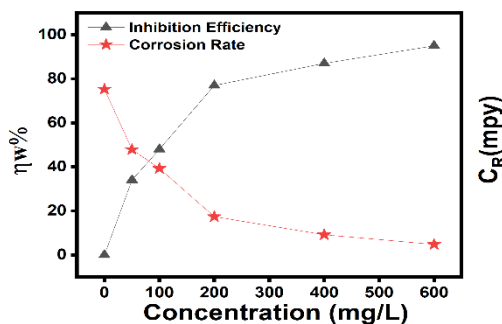


Figure 3. Inhibition efficiency and corrosion rate depicted for mild steel in 0.5M sulfuric acid at different concentration of the inhibitor.

3.2. Electrochemical Investigation

3.2.1. Electrochemical impedance spectroscopy (EIS)

Impedance studies with different concentrations of ECBF inhibitor in 0.5M sulfuric acid were done to evaluate the greatest charge transfer resistance in contrast to a blank (0.5M sulfuric acid without inhibitor). The impedance data are shown using Nyquist (Fig. 4a), Bode (Fig. 4b), and Phase angle (Fig. 4c) graphs. Low semicircles may be detected in the medium frequency zone when the axes of the x and y axes have the same value as one another.

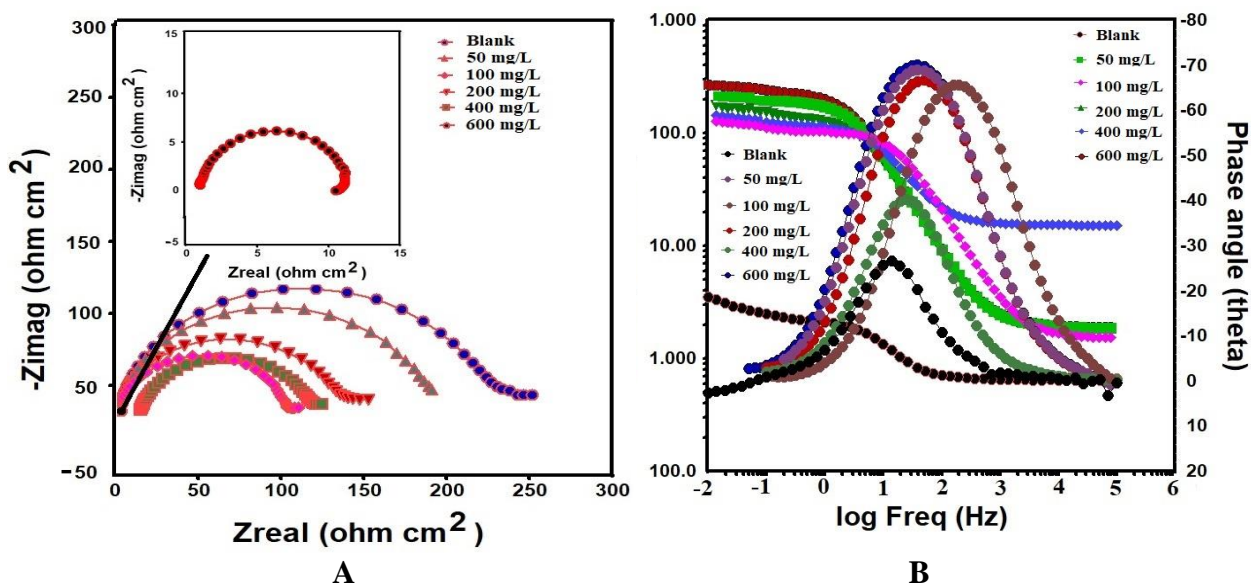


Figure 4. (a) Nyquist plot of ECBF in sulfuric acid solution and (b) Bode and phase angle plots for mild steel in sulfuric acid solution.

In aggressive media, the Nyquist plots all had the same shape because the corrosion process was equal; as a result, the corrosion process was equivalent [16]. As the ECBF concentration grew, the charge transfer resistance (R_{ct}) increased, as assessed by the length of the Nyquist graphs. This effect is

responsible for the excellent steel corrosion mitigation by ECBF inhibitor in 0.5M sulfuric acid [17, 18]. With increasing ECBF concentration, the slope values tend to shift to unity, as seen in Bode plots (Fig. 4b). The phase angle graphs (Fig. 4b) followed the same trend, with peak values rising as the angle neared 80 degrees.

Table 1. Standard deviation (SD) of mild steel electrochemical impedance characteristics in sulfuric acid solution at various inhibitor concentrations.

| C_{inh} (mg/L) | R_s (Ωcm^2) | R_{ct} (Ωcm^2) | $Y0^*$ ($\Omega^{-1}s^n/cm^2$) | n | $-S$ | α ($^\circ$) | η_{EIS} (%) |
|---------------------|----------------------------|-------------------------------|-------------------------------------|-------|-------|--------------------------|---------------------|
| Blank | 1.9 | 10.1± 0.003 | 297.4 | 0.559 | 0.478 | 29.8 | -- |
| 50 | 1.7 | 96.5± 0.033 | 178.6 | 0.688 | 0.517 | 40.2 | 89.5 |
| 100 | 1.5 | 105.9± 0.007 | 199.4 | 0.732 | 0.565 | 61.2 | 90.4 |
| 200 | 1.4 | 137.9± 0.043 | 107.4 | 0.737 | 0.597 | 63.1 | 92.6 |
| 400 | 1.8 | 191.3± 0.001 | 177.2 | 0.834 | 0.646 | 66.4 | 94.7 |
| 600 | 1.9 | 245.3± 0.021 | 189.2 | 0.876 | 0.687 | 67.9 | 95.8 |

The steepest incline was 0.687 degrees, and the highest point was 67.9 degrees above sea level. Mild steel under corrosive circumstances had the maximum slope value of 0.687 and the highest peak angle of 67.9° when exposed to 600 mg/L ECBF concentration. The rise in steel resistance is responsible for these changes in values as well as the tendency to approach the maximum. The ECBF molecules, which form a protective coating on the steel surface, are responsible for the increased resistance [19]. The effect is caused by the adsorption of ECBF molecules on the steel surface.

The obtained data was analyzed using the relevant model in the Echem analyzer programme (Fig. 5), and the findings are shown in Table 1. After three repeated testing, the model fits the graph incredibly well, and the standard deviation has been reduced, indicating that the model is well-fitting to the data.

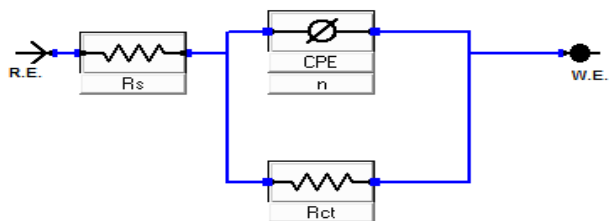


Figure 5. Equivalent circuit used to fit the Nyquist plots.

In the model, a constant phase element (CPE), a charge transfer resistance (R_{ct}), and the solution resistance (R_s) are all included as components. CPE was previously used in place of a pure capacitor to get a good match and precise comparable results in earlier experiments. The CPE impedance was premeditated using the equation below:

$$Z_{CPE} = Y_0 [j\omega^\alpha]^{-1} \tag{4}$$

where j be the complex value ($j = \sqrt{-1}$), Y_0 be the admittance and invariant for CPE, ω be the angular frequency in rad/s and α , be the phase shift [20]. Through adsorption on the steel/solution intersection, the ECBF molecules raise the resistance and influence the property of the pure capacitor.

Table 1 shows that when R_{ct} values rise, so does the ECBF inhibitor's inhibitory activity in a 0.5M sulfuric acid solution. Changing the homogeneity of the solution and changing the interface between the metal and solution, lead to a tendency for the values of phase change (n) to decrease and eventually reach unity. This is due to the surface absorption of ECBF molecules on mild steel, which prevents corrosive medium from penetrating the steel [21].

3.2.2. Electrochemical frequency modulation (EFM)

EFM is a useful approach for measuring corrosion rate and efficiency in a short length of time without the need for previous knowledge of Tafel constants, which is advantageous [22]. Experiments with EFM yielded the following frequency and intermodulation spectra, which are shown in Figure 6.

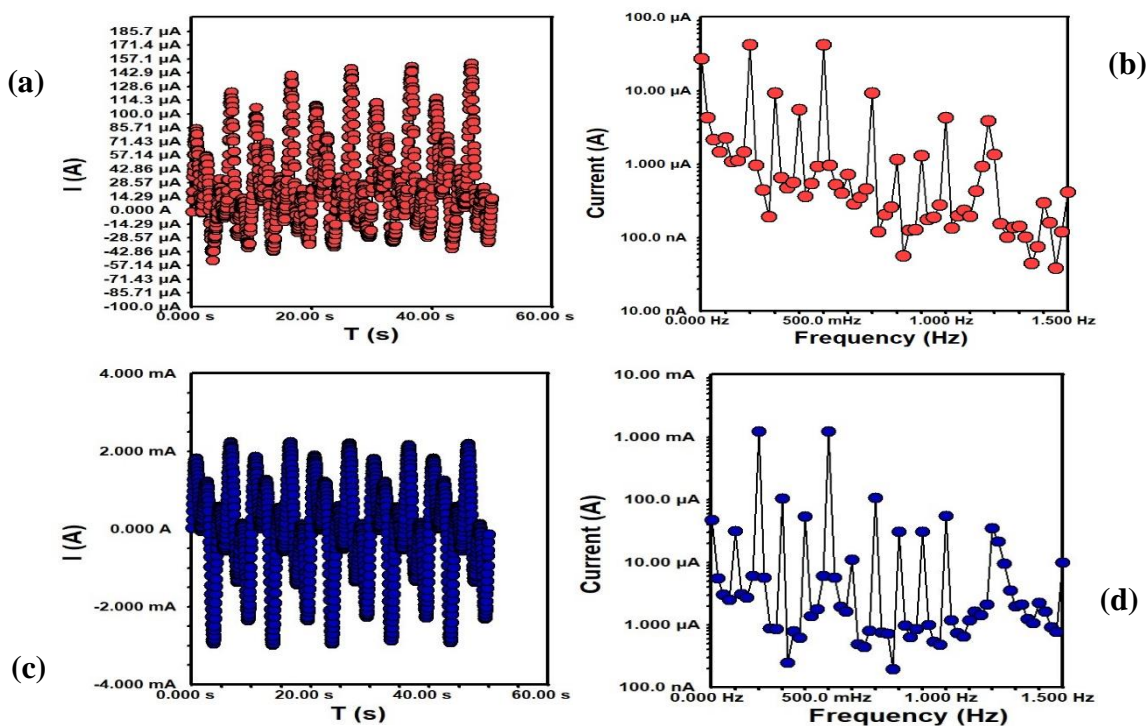


Figure 6. (a) Electrochemical frequency modulation curves for Blank + mild steel and (b) Intermodulation curves for Blank + mild steel (c) Electrochemical frequency modulation curves for inhibitor + mild steel and (d) Intermodulation curves for inhibitor + mild steel in sulfuric acid solution.

Table 2. Electrochemical frequency modulation parameters for mild steel in 0.5M sulfuric acid solution.

| | i_{corr} ($\mu\text{A}/\text{cm}^2$) | β_a (mV/dec) | $-\beta_c$ (mV/dec) | CF-2 | CF-3 | η_{EFM} (%) |
|-------|---|-----------------------|------------------------|-------|-------|---------------------|
| Blank | 1432.9 | 94 | 141 | 1.942 | 3.072 | -- |
| ECBF | 56.7 | 54 | 212 | 1.997 | 2.918 | 96.0 |

Table 2 shows the analyzed values of the studied inhibitor in 0.5M sulfuric acid. The corrosion current density (i_{corr}) of the corrosive medium is higher, whereas that of the ECBF-inhibited solution is lower. The casualty factors 2 and 3 are in accordance with and perfectly equivalent to the hypothetical variables of the published EFM notion [23], as shown in Table 2. The equation below was utilized to calculate the inhibition efficiency ($\eta_{EFM}\%$) using the i_{corr} values.

$$\eta_{EFM} \% = \left(1 - \frac{i_{corr}^{inh}}{i_{corr}^{blank}} \right) \times 100 \tag{5}$$

where i_{corr}^{blank} and i_{corr}^{inh} be the corrosion current densities in the absence and presence of the studied inhibitor, respectively. At 600 mg/L concentration, the ECBF inhibitor showed a 96 percent inhibitory effectiveness.

3.2.3. Potentiodynamic polarization (PDP)

To produce the PDP curves, polarization tests were done using 0.5M sulfuric acid in the absence and presence of ECBF inhibitor (Fig. 7). Table 3 shows the values of several parameters extrapolated from the graph.

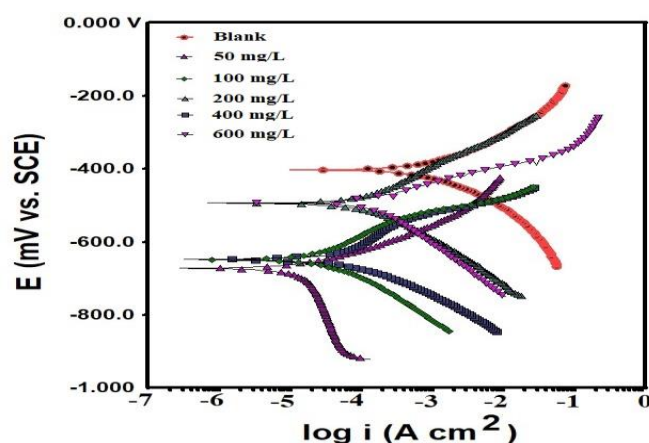


Figure 7. Potentiodynamic polarization curves for mild steel in sulfuric acid solution.

Table 3 suggests that as the amount of ECBF inhibitor increases, the amount of i_{corr} decreases. In this case, the adsorption of ECBF molecules on the steel surface results in the formation of a protective layer over active corrosion centers, preventing the entry of sulfuric acid solution. However,

despite the fact that both the cathodic and anodic sections have been modified, there is still a large cathodic dominance present.

Table 3. Potentiodynamic polarization parameters of mild steel in 0.5M sulfuric acid solution with standard deviation (\pm SD) at different concentration of the inhibitor.

| Inhibitor (mg/L) | E_{corr} (mV/SCE) | i_{corr} ($\mu\text{A}/\text{cm}^2$) | β_a (mV/dec) | $-\beta_c$ (mV/dec) | η_{PDP} (%) |
|---------------------|-------------------------------|--|-----------------------|------------------------|----------------------------|
| Blank | -369 | 158.3 \pm 0.016 | 109 | 64 | -- |
| 50 | -403 | 102.1 \pm 0.016 | 70 | 74 | 35.5 |
| 100 | -495 | 33.5 \pm 0.056 | 97 | 153 | 78.8 |
| 200 | -649 | 26.2 \pm 0.047 | 69 | 100 | 83.4 |
| 400 | -649 | 19.1 \pm 0.016 | 107 | 71 | 87.9 |
| 600 | -672 | 11.7 \pm 0.012 | 71 | 106 | 92.6 |

When comparing the E_{corr} values for ECBF inhibitor to those for sulfuric acid solution, it is clear that the motions are much different. In aggressive medium, ECBF inhibitor revealed a peak inhibitory efficacy of 92.6 percent when administered at 600 mg/L. According to [24], the efficiency gained is sufficient for a possible corrosion inhibitor. It has been shown that the film created by electrochemical bonding serves as a barrier to the flow of electrons engaged in redox processes, affecting the kinetics of the electrochemical reactions involved [25].

3.2. Surface analysis

3.2.1. Scanning electron microscopy (SEM)

Both a blank sulfuric acid solution and a 600 mg/L ECBF inhibitor solution were used to treat the mild steel. After cleaning and vacuum drying, the steel was placed in front of the machine for surface tests, as seen in Fig. 8.

The surface of mild steel looks rough, cracked, and corroded without ECBF in sulfuric acid (Fig. 8a). It's possible that this is due to the aggressive media creating a fast dissolving response at the electrode. In the same aggressive medium, a coating of ECBF was applied to the mild steel surface, which seemed to be less corroded, undamaged, and smooth (Fig. 8b). When the steel was abraded, the lines were hardly visible, and the mirror shine was destroyed by the action of sulfuric acid [25].

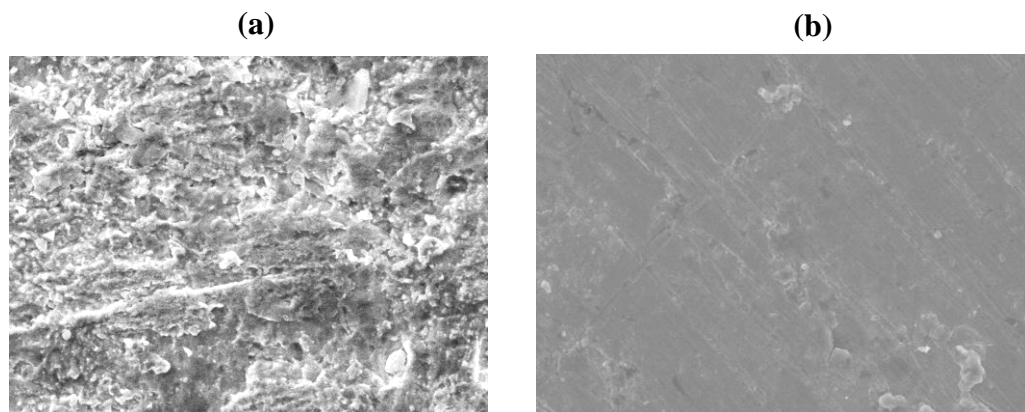


Figure 8. SEM micrographs of mild steel in (a) in sulfuric acid solution, and (b) inhibited solution.

3.2.2. Atomic Force microscopy (AFM)

To get 2D/3D surface pictures, the mild steel coupons were treated to the AFM machine. These 3D photographs may show a distinct texture of the surface as well as roughness, as seen in Fig. 9. Mild steel has a rough and deteriorated surface in sulfuric acid without the ECBF inhibitor (Fig. 9a).

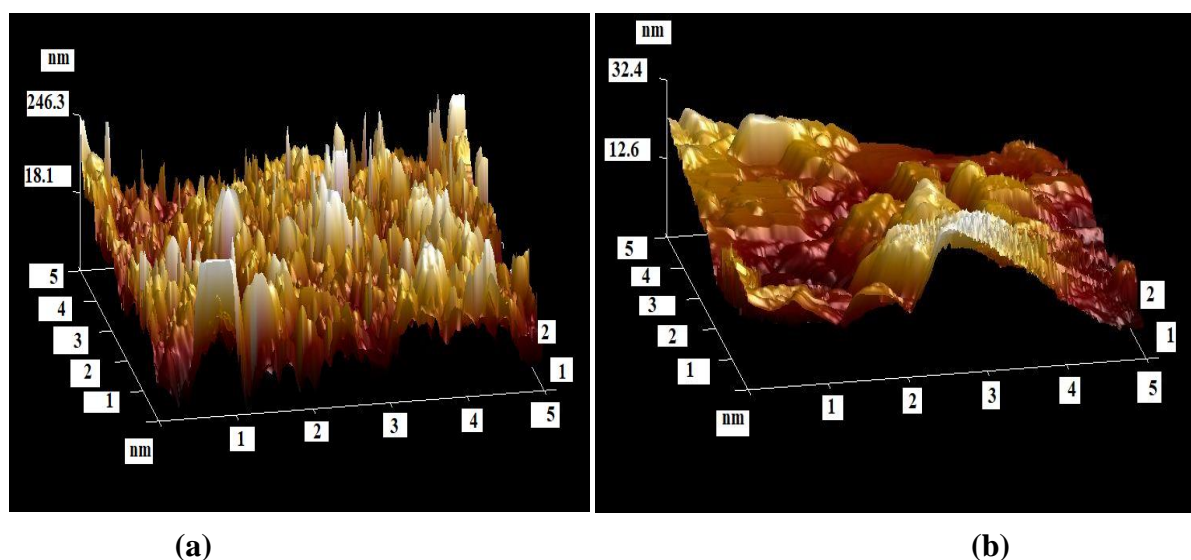


Figure 9. AFM micrographs of mild steel in (a) in sulfuric acid solution, and (b) inhibited solution.

The steel had a roughness of 246.3 nm, as illustrated in Fig. 9a. The roughness of mild steel in sulfuric acid with ECBF inhibitor (600 mg/L) was 32.4 nm, as shown in Fig. 9b. The formation of a tight link between the steel surface and the ECBF inhibitor may be responsible for the decrease in roughness [26, 27].

4. CONCLUSIONS

1. A higher dose of 600 mg/L ECBF demonstrated a 95 percent inhibitory effectiveness in sulfuric acid.
2. R_{ct} values are increased in the presence of ECBF inhibitor, according to the impedance research.
3. The main cathodic shift was revealed by analyzing the polarization curves.
4. The smooth surface for mild steel with ECBF layer and corroded without ECBF inhibitor was shown in SEM and AFM images.

References

1. A. Singh, K.R. Ansari, Abdullah K. Alanazi, M.A. Quraishi and Priyabrata Banerjee, *J. Mol. Liq.*, 345 (2022) 117866.
2. Ekemini Ituen, A. Singh, Lin Yuanhua and Onyewuchi Akaranta, *Cleaner Eng. Tech.*, 3 (2021) 100119.
3. A. Singh, K. Ansari, A. Kumar, W. Liu, C. Songsong and Y. Lin, *J. Alloy. Compd.*, 712 (2017) 121.
4. G. Quartarone, M. Battilana, L. Bonaldo and T. Tortato, *Corros. Sci.*, 50 (2008) 3467.
5. A. Singh, K. R. Ansari, D. S. Chauhan, M. A. Quraishi, H. Lgaz and I. M. Chung, *J. Colloid Interface Sci.*, 560 (2020) 225.
6. Rouhollah Sabzi and Reza Arefinia, *Corros. Sci.*, 153 (2019) 292.
7. Ambrish Singh, K.R. Ansari, M.A. Quraishi, Savaş Kaya and Sultan Erkan, *Int. J. Hydrogen Energy*, 46 (2021) 9452.
8. Shivani Singh, Rahul Singh, Neeta Raj Sharma, A. Singh, *Int. J. Electrochem. Sci.* 16 (2021) 210841.
9. Peng Su, Lintao Li, W. Li, C. Huang, X. Wang, H. Liu and A. Singh, *Int. J. Electrochem. Sci.*, 15 (2020) 1412.
10. A. Singh, K.R. Ansari, J. Haque, P. Dohare, H. Lgaz, R. Salghi and M.A. Quraishi, *J. Taiwan Inst. Chem. E.*, 82 (2018) 233.
11. ASTM G31-72 Standard Practice for Laboratory Immersion Corrosion Testing of Metals; ASTM International: West Conshohocken, PA, USA, 2004.
12. K.R. Ansari, M.A. Quraishi and Ambrish Singh, *Corros. Sci.*, 79 (2014) 5.
13. Ambrish Singh, Yuanhua Lin, K. R. Ansari, M. A. Quraishi, Eno. E. Ebenso, Songsong Chen and Wanying Liu, *Appl. Surf. Sci.*, 359 (2015) 331.
14. S. A. Haddadi, E. Alibakhshi, G. Bahlakeh, B. Ramezanzadeh and M. Mahdavian, *J. Mol. Liq.*, 284 (2019) 682.
15. A. Singh, K.R. Ansari, A. Kumar, W. Liu, C. Songsong and Y. Lin, *J. Alloy Compd.*, 712 (2017) 121.
16. K Habib and K Muhana, *Electrochem. Commun.*, 4 (2002) 54.
17. M. Ramezanzadeh, Z. Sanaei, G. Bahlakeh and B. Ramezanzadeh, *J. Mol. Liq.*, 256 (2018) 67.
18. K. R. Ansari, Dheeraj Singh Chauhan, M. A. Quraishi, Mohammad A. J. Mazumder and A. Singh, *Int. J. Biological Macromol.*, 1441 (2020) 305.
19. Yang Yaocheng, Yin Caihong, A. Singh and Yuanhua Lin, *New. J. Chem.*, 43 (2019) 16058.
20. Qingyang Li, Wei Li and Maozhong An, *Electrochem. Commun.*, 90 (2018) 39.
21. Qiongyu Zhou, Saad Sheikh, Ping Ou, Dongchu Chen and Sheng Guo, *Electrochem. Commun.*, 98 (2019) 63.
22. A. Singh, K. R. Ansari, X. Xu, Z. Sun, A. Kumar and Y. Lin, *Sci. Rep.*, 7 (2017) 14904.

23. Jun Zhao, Ningsheng Zhang, Chengtun Qu, Xinmin Wu, Juantao Zhang and Xiang Zhang, *Ind. Eng. Chem. Res.*, 49 (2010) 3986.
24. Ambrish Singh, I Ahamad, V. K. Singh and M. A. Quraishi, *J. Sol. State Electrochem.*, 15 (2011) 1087.
25. A. Singh, K.R. Ansari, M.A. Quraishi, H. Lgaz and Y. Lin, *J. Alloy Compd.*, 762 (2018) 347.
26. A. Nazarov, M. G. Olivier and D. Thierry, *Prog. Org. Coat.* 74 (2012) 356.
27. A. Singh, Hazem Samih Mohamed, Shivani Singh, Hua Yu and Yuanhua Lin, *Constr. Build. Mater.*, 258 (2020) 119728.

© 2022 The Authors. Published by ESG (www.electrochemsci.org). This article is an open access article distributed under the terms and conditions of the Creative Commons Attribution license (<http://creativecommons.org/licenses/by/4.0/>).